



# Journal of Hunan University (Natural Sciences)

Vol. 53 No. 3

March 2026

Available online at

<https://joununs.com>



ELSEVIER  
Scopus



Clarivate  
WEB OF SCIENCE

Open Access Article

 <https://doi.org/10.55463/issn.1674-2974.53.3.1>

## Data-Driven Explainable Machine learning for Rockburst Hazard and Seismic Resilience with 3D Fragility Surfaces

Mozumder Mohibullah<sup>\*1</sup>, Longjun Dong<sup>1</sup>, Abdul Ahad Hassan Farroqi<sup>2</sup>, Labanyo Barcher<sup>1</sup>,  
Hossen MD Walid<sup>3</sup>

<sup>1</sup>School of Resource and Safety Engineering, Central South University, Changsha, China,

<sup>2</sup>School of Economics and Trade, Hunan University, Changsha, China,

<sup>3</sup>School of Mines, China University of Mining and Technology, Xuzhou, Jiangsu, China,

\* Corresponding author: [mohibullahrabby@gmail.com](mailto:mohibullahrabby@gmail.com)

### Article History:

Received: January 27, 2026

Revised: February 24, 2026

Accepted: March 5, 2026

Published: March 31, 2026

**Abstract:** Rockbursts are critical geohazards in deep underground mining and tunneling and can cause catastrophic structural failures, severe safety risks, and substantial economic losses. Owing to their nonlinear and spatiotemporally variable behavior, conventional microseismic monitoring approaches often provide limited predictive capability.

This study proposes a data-driven machine learning (ML) framework to model rockburst fragility surfaces and assess seismic resilience under complex geological conditions. The workflow begins with preprocessing of in-situ monitoring data, including dimensionality reduction, feature engineering, and normalization to enhance data quality and relevance. Multiple ML algorithms, including XGBoost, Random Forest, LightGBM, and CatBoost, are trained using labeled datasets representing moderate-to-severe rockburst events.

To improve robustness and generalization, an ensemble voting classifier is developed, with hyperparameters optimized using grid search and evolutionary optimization. The framework maintains strong predictive consistency even for imbalanced datasets. Feature importance analysis identifies seismic energy release and ground stress as the dominant predictors of rockburst occurrence.

Using these insights, the model generates three-dimensional fragility surfaces that characterize structural



Copyright: © 2026 by the authors. Licensee JHU

This article is an open-access article distributed under the terms and conditions of the Creative Commons Attribution License  
<http://creativecommons.org/licenses/by/4.0/>

vulnerability under varying seismic loads, along with probabilistic fragility curves that delineate risk zones to support early-warning systems and real-time operational decision-making. By integrating physics-informed assessment with explainable ML, the proposed approach improves interpretability while meeting practical engineering requirements.

Overall, this study provides a scalable, high-performance framework for seismic resilience analysis, enabling improved hazard prediction, risk management, and the design of safer underground systems in complex geomechanical environments.

**Keywords:** Rockburst; Seismic resilience; Machine learning; Fragility curve; Hazard prediction; Seismic risk assessment; Ensemble learning; 3D fragility surfaces; Explainable AI.

## 数据驱动的可解释机器学习在岩爆危险性与地震韧性评估中的应用：基于三维脆弱性曲面的方法

**摘要：**岩爆是深部地下采矿与隧道工程中的一种关键地质灾害，可能导致灾难性结构破坏、严重安全风险以及巨大的经济损失。由于岩爆过程具有显著的非线性和时空变异性，传统的微震监测方法往往难以提供有效的预测能力。

本研究提出了一种数据驱动的机器学习（ML）框架，用于构建岩爆脆弱性曲面并评估复杂地质条件下的地震韧性。该研究流程首先对原位监测数据进行预处理，包括降维、特征工程和数据归一化，以提高数据质量和相关性。随后采用多种机器学习算法，包括 XGBoost、

Random Forest、LightGBM 和 CatBoost，并利用标注数据集对中到强烈岩爆事件进行训练

为提高模型的稳健性与泛化能力，构建了集成投票分类器，并通过网格搜索与进化优化方法对超参数进行优化。该框架即使在数据集不平衡的情况下仍保持较高的预测一致性。特征重要性分析表明，地震能量释放与地应力是岩爆发生的主要预测因子。

基于上述分析结果，模型进一步生成三维脆弱性曲面，以表征不同地震载荷条件下结构的脆弱性，并构建概率脆弱性曲线，用于划分风险区域，从而支持预警系统与实时运行决策。通过将基于物理机理的评估方法与可解释机器学习相结合，该方法在满足工程实际需求的同时提高了模型的可解释性。

总体而言，本研究提出了一种具有良好可扩展性和高性能的地震韧性分析框架，可用于提升灾害预测能力、风险管理水平以及复杂地质环境下地下工程系统的安全设计。

**关键词：**地震韧性，机器学习，脆弱性曲线，灾害预测，地震风险评估，集成学习，三维脆弱性曲面，可解释人工智能。

### 1. Introduction

Rockbursts are among the most critical geohazards in deep underground mining and tunneling, where sudden and violent rock mass failure can lead to severe damage to excavations and support systems, endanger worker safety, disrupt production, and cause substantial economic losses [1]. With increasing excavation depth and more complex in-situ stress environments, the frequency and intensity of rockburst-related hazards may rise, making reliable monitoring, prediction, and risk mitigation essential for safe and sustainable underground operations.

Microseismic monitoring has become a widely adopted technique for detecting rock fracturing and

instability in real time, offering valuable insights into stress redistribution and damage evolution within rock masses [2]. However, although microseismic systems are highly effective for event detection and post-event interpretation, they are still often used in a reactive manner and may provide limited predictive capability for imminent rockburst occurrence [3]. This challenge is largely driven by the nonlinear and spatiotemporally variable relationships among geological structures, excavation-induced stress changes, seismic energy release, and dynamic responses of the surrounding rock mass. Traditional empirical and physics-based approaches frequently struggle to represent these complex multivariate interactions in evolving

underground conditions [4,5]. Consequently, there is a strong need for data-driven methods that can learn these relationships directly from monitoring data while remaining usable for engineering decisions.

Conventional rockburst prediction approaches primarily include empirical criteria, rule-based expert systems, statistical regression, and probabilistic methods. Empirical techniques rely on indicators such as in-situ stress, rock strength, and excavation depth, but their applicability is often limited by small datasets and poor generalizability across diverse geological settings [11]. Rule-based expert systems encode expert knowledge using predefined logical rules (e.g., rock type, tunnel geometry), yet they can be rigid and less effective under complex or changing conditions [12]. Statistical models such as linear and logistic regression provide simple interpretable formulations, but they often assume linearity and have difficulty capturing nonlinear or multivariate interactions [13]. Probabilistic and Bayesian frameworks can incorporate uncertainty by combining prior information with current observations, but they can be sensitive to prior selection, require sufficient data for reliable inference, and may become computationally intensive as input dimensionality increases [14]. These limitations motivate the use of machine learning methods that can model complex nonlinear patterns and interactions more flexibly.

In recent years, machine learning (ML) has shown strong potential for rockburst prediction because it can extract hidden patterns from high-dimensional microseismic datasets and integrate multiple seismic indicators into a unified predictive model [6]. Prior studies have applied nonlinear SVM models for identifying rockburst-related patterns from microseismic data [15], while Random Forest models have demonstrated robust prediction performance across various datasets and geological contexts [16–18]. Gradient boosting approaches have also been effective for noisy and imbalanced data commonly encountered in rock engineering applications [19]. Ensemble learning strategies (e.g., stacking and voting) can further improve robustness and generalization by combining complementary strengths from multiple learners [20]. Nevertheless, several challenges remain: (i) rockburst datasets are often imbalanced, where severe events are rare relative to normal or low-risk states, which can bias learning and reduce reliability for high-consequence predictions [21]; (ii) many high-performing ML models have limited interpretability and may be perceived as “black boxes,” restricting their acceptance in safety-critical engineering workflows [7]; and (iii) site-specific training and limited samples can hinder transferability to unseen geological conditions, particularly for complex deep learning architectures [22,23].

To address interpretability concerns, explainable artificial intelligence (XAI) has increasingly been adopted to provide transparent reasoning for ML

predictions. Model-agnostic explanation methods such as LIME and SHAP can quantify how input variables influence outputs at both local and global levels, supporting validation, debugging, and decision-making in practice [7,40]. From an engineering perspective, interpretability is especially important because it helps connect model outputs to physical understanding such as the roles of seismic energy release and stress state thereby improving trust and operational usability. In addition, robust prediction in real monitoring conditions requires careful preprocessing to improve data quality and relevance, including outlier treatment, normalization/standardization, dimensionality reduction, and feature engineering. It also requires systematic hyperparameter optimization (e.g., grid search and evolutionary strategies) to improve stability and generalization under noisy and imbalanced datasets.

Beyond predicting whether a rockburst may occur, modern risk management increasingly emphasizes seismic resilience evaluating how underground systems resist damage and maintain functionality under varying seismic demands. Fragility analysis provides a probabilistic framework that relates seismic intensity measures to the probability of exceeding specified damage states, enabling risk zoning and vulnerability-informed design and operation [9,10]. Recent research has demonstrated that fragility curves and three-dimensional fragility surfaces can enhance seismic vulnerability assessment for underground and structural systems by capturing nonlinear interactions among multiple seismic parameters [24,25]. For underground mining and tunneling, a data-driven fragility surface is particularly valuable because it can map risk as a function of key seismic indicators (e.g., magnitude- and frequency-related parameters) while reflecting the combined influence of multiple features, thereby supporting early warning and real-time operational decisions.

Accordingly, this study proposes a data-driven, physics-informed ML framework for rockburst prediction and seismic resilience assessment by generating probabilistic fragility curves and three-dimensional fragility surfaces from in-situ monitoring data. Multiple ML algorithms (including boosting and bagging-based models) are trained to classify moderate-to-severe rockburst occurrence, and an ensemble voting strategy is adopted to enhance robustness and generalizability under imbalanced conditions. Hyperparameters are optimized using systematic search and evolutionary optimization, and XAI methods are integrated to identify dominant predictors and improve transparency. The primary contributions of this work are:

1. Development of ML-based rockburst prediction models using microseismic and stress-related indicators.
2. Construction of a voting-based ensemble classifier to improve robustness and generalization for

imbalanced datasets.

3. Integration of XAI methods to interpret model behavior and identify key predictors (e.g., seismic energy release and stress state).

4. Generation of probabilistic fragility curves and 3D fragility surfaces to support seismic resilience assessment, risk zoning, and operational decision-making.

The remainder of this paper is organized as follows: Section 2 describes the dataset and methodology, including preprocessing, model training, and fragility surface construction. Section 3 presents predictive performance and resilience-related results. Section 4 discusses key findings, limitations, and future research directions.

## 2. Methodology

Headings should be of three-level type. This study proposes a data-driven machine learning (ML) workflow for rockburst prediction and seismic resilience assessment through probabilistic fragility analysis. The overall framework includes: (i) dataset preparation and exploratory analysis, (ii) preprocessing and feature engineering, (iii) supervised model development using multiple ML algorithms, (iv) hyperparameter optimization, (v) evaluation using standard classification metrics, (vi) explainable AI (XAI) for interpretability, and (vii) construction of a three-dimensional (3D) fragility surface to visualize rockburst probability under varying seismic conditions.

### 2.1. Dataset and Exploratory Analysis

A dataset of seismic/microseismic event recordings was collected from an underground excavation site. The variables represent key indicators commonly used in rockburst prediction and include: Average Wave Velocity, Corner Frequency, Seismic Event Count, Seismic Energy, Peak Speed, Peak Acceleration, Richter Scale Magnitude, and Moment Magnitude. Exploratory data analysis (EDA) was conducted to examine the statistical distribution of each feature and to understand inter-feature relationships before model training.

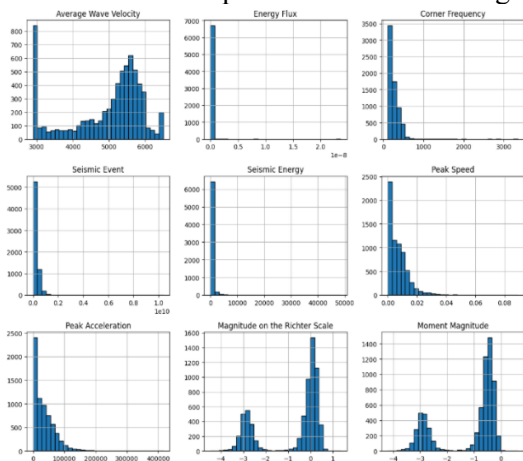
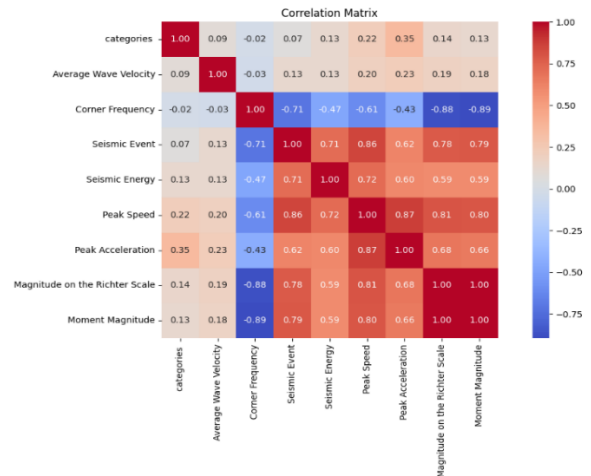


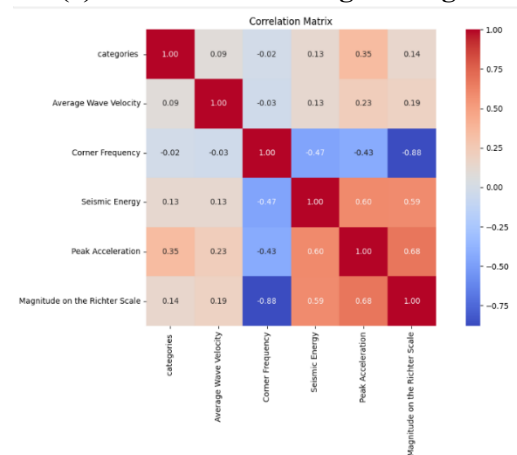
Figure 1: Feature Distribution. (Developed by Authors)

The feature distributions indicate that high-value outliers are present in most variables. Several features (e.g., seismic energy, peak speed, peak acceleration, and corner frequency) are strongly right-skewed, and moment magnitude and Richter scale magnitude show multimodal behavior, which may reflect clustering across different seismic activity regimes. These non-normal distributions motivate preprocessing steps such as outlier treatment and feature scaling.

To quantify the linear dependency structure among features, a Pearson correlation matrix was computed.



(a) Before Feature Engineering



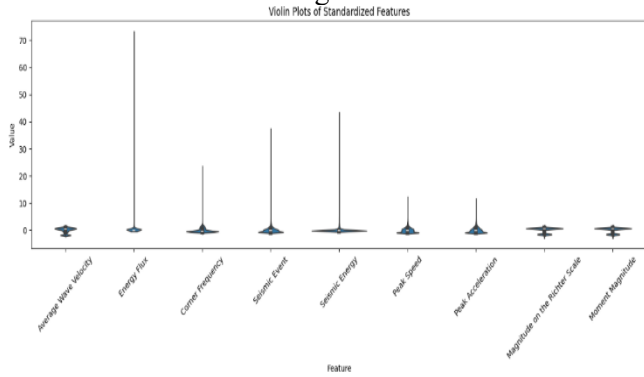
(b) After Feature Engineering

Figure 2: Correlation Matrix (a) Before Feature Engineering, (b) After Feature Engineering. (Developed by Authors)

The correlation analysis reveals strong dependence among several variables, particularly between magnitude- and acceleration-related indicators, indicating multicollinearity risk. Corner frequency shows notable negative correlation with energy-related measures, suggesting that frequency-based information provides complementary content for prediction. The correlation structure guides feature selection to reduce redundancy and improve model generalization.

### 2.2. Preprocessing

Before model training, a comprehensive preprocessing pipeline was implemented to enhance data quality and improve predictive performance. First, missing values and irrelevant or non-informative features were identified and removed using domain knowledge and EDA. Next, outliers were detected visually using violin plots and treated using the interquartile range (IQR) criterion. Specifically, observations beyond  $1.5 \times \text{IQR}$  below the lower quartile or above the upper quartile were classified as outliers and handled to reduce their influence on model learning.



**Figure 3: Violin Plot for Outliers. (Developed by Authors)**

Feature scaling was then applied to ensure uniform scaling across variables. Both standardization (z-score normalization) and min-max normalization were used, depending on algorithm sensitivity: normalization benefits models that perform better with bounded inputs, while standardization is appropriate for variance-sensitive learning. These preprocessing steps support stable optimization, reduce training instability, and improve interpretability during modeling.

**2.3. Supervised Learning Formulation and Training Strategy**

Rockburst prediction was formulated as a supervised classification problem, where the target is to predict the rockburst intensity class from observed seismic indicators [27]. The dataset was divided into training and testing subsets to ensure robust development and unbiased evaluation. During training, the model learns from the training subset after preprocessing and feature selection, with additional techniques such as clustering and advanced feature selection used when required to extract the most relevant seismic indicators [28]. Hyperparameter tuning was conducted using optimization strategies such as grid search cross-validation, which explores the parameter space to identify configurations that maximize predictive accuracy.

In this study, the dataset was split into 70% training and 30% testing, respectively. Model performance was then evaluated on unseen test data using standard classification metrics such as precision, F1-score, and confusion-matrix-based measures. This structured process aligns with recent comparative studies and

reviews of AI-based rockburst prediction frameworks [29,30].

**2.4. Machine Learning Models**

The ML algorithms used in this work include ensemble learning methods (bagging, boosting, and voting) and a neural network model. These approaches are widely applied in rockburst prediction because they can capture nonlinear relationships among seismic indicators and provide improved generalization compared with single-model approaches [26].

**2.4.1. Bagging (Bootstrap Aggregating)**

Bagging is an ensemble technique that improves model stability by reducing variance. It is particularly effective for high-variance base learners such as decision trees. Bagging trains multiple learners on bootstrapped subsets of the training data and aggregates predictions, reducing overfitting by averaging out noise across learners [31]. Random Forest is a bagging-based method that also applies random feature selection at each split to reduce correlation among trees and improve generalization [32].

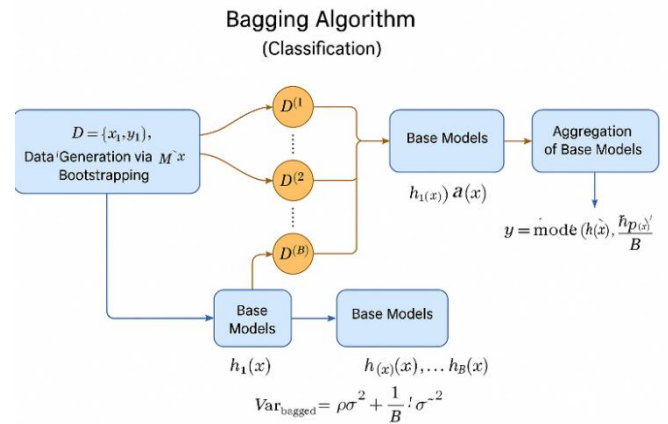


**Figure 4: Bagging ensemble learning framework. (Developed by Authors)**

$$D = \{(x_1, y_1), (x_2, y_2), \dots, (x_n, y_n)\} \tag{1}$$

B bootstrap samples are generated as:

$$D^{(1)}, D^{(2)}, \dots, D^{(B)} \tag{2}$$

For a new input x, the bagging prediction is obtained by majority voting:

$$\hat{y}_{\text{bag}}(x) = \text{majority vote}(h_1(x), h_2(x), \dots, h_B(x)) \tag{3}$$

**2.4.2. Boosting**

Boosting is a sequential ensemble approach where each learner focuses on correcting the errors of previous learners. Boosting algorithms such as AdaBoost and XGBoost can achieve strong performance for rockburst classification and are particularly useful for difficult and imbalanced cases because they increase the weight of misclassified samples during training [28]. The final

boosted prediction is obtained by combining weak learners using weighted aggregation.

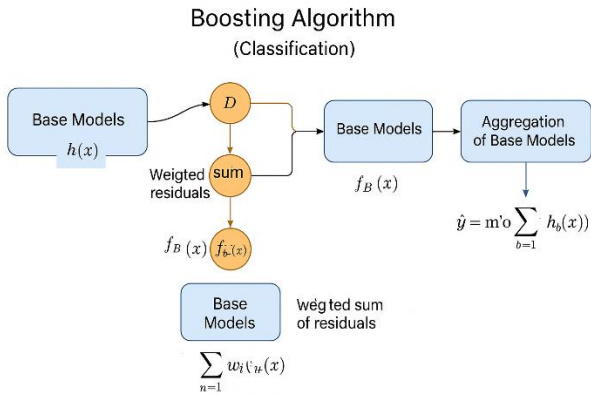


**Figure 5: Boosting ensemble learning framework. (Developed by Authors)**

2.4.3. Voting Classifier (Heterogeneous Ensemble)

Voting classifiers are effective for aggregating predictions from models trained on different feature representations [33]. In rockburst prediction, voting can combine methods such as XGBoost, SVM, CatBoost, and Random Forest to reduce weaknesses of individual learners and improve generalization [34].

Two voting strategies are used:

- **Hard voting:** selects the final class label by majority rule.
- **Soft voting:** averages predicted class probabilities (optionally weighted) and selects the class with the maximum combined probability.

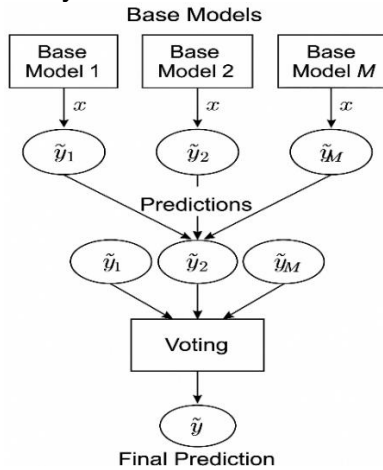


**Figure 6: Voting Classifier visualization. (Developed by Authors)**

$$\hat{y}(x) = \operatorname{argmax}_c \sum_{k=1}^K w_k P_k(y = c | x) \quad (5)$$

Soft voting (probability-based) is defined as:

$$\hat{y}(x) = \operatorname{argmax}_c \sum_{k=1}^K w_k P_k(y = c | x) \quad (6)$$

2.4.4 Neural Network

A neural network is a computational model composed of interconnected layers (input, hidden, output) that learns nonlinear mappings through optimization of weights and biases. After receiving inputs, each neuron computes a weighted sum and applies an activation function (e.g., sigmoid or ReLU) before passing the result forward. Neural networks can represent complex relationships and extract hierarchical features, although deeper architectures may be needed for challenging prediction tasks [35].

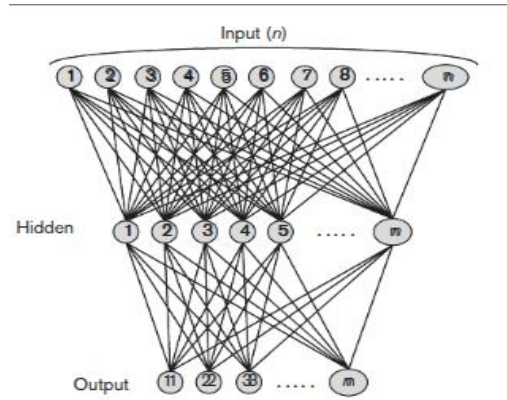


**Figure 7: Backpropagation Neural Network Architecture [36].**

2.4.5 Proposed Voting-Based Rockburst Prediction Framework

A hybrid voting-based prediction framework is adopted to integrate preprocessing, feature extraction, hyperparameter tuning, and ensemble learning. Multiple base models are trained using cross-validation and grid-search tuning, then combined through ensemble voting to improve robustness. If performance is unsatisfactory, feature importance is analyzed and physics-informed feature refinement is applied to improve input representations, forming an iterative feedback loop.

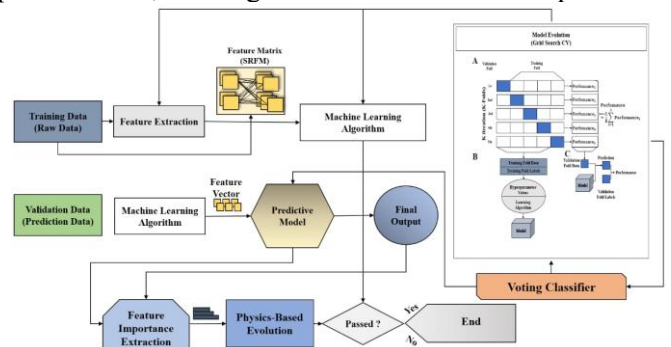


**Figure 8: Proposed framework for data-driven ML modeling of rockburst fragility surfaces in seismic resilience analysis. (Developed by Authors)**

$$\hat{y} = \operatorname{MajorityVote}(f_1(x), f_2(x), \dots, f_n(x)) \quad (7)$$

2.5 Hyperparameter Optimization

Hyperparameter tuning aims to optimize model accuracy by selecting values for predefined

configurations such as learning rate, tree depth, regularization parameters, and number of estimators. Since these are not learned directly from the data, optimization techniques such as grid search cross-validation are used to explore candidate configurations and select the best-performing settings. This step reduces underfitting/overfitting risk and improves model generalization.

## 2.6 Performance Measurement and Evaluation

Model performance was evaluated using confusion-matrix definitions: TP (true positives), TN (true negatives), FP (false positives), and FN (false negatives). Standard classification metrics were computed:

$$Accuracy = (TP + TN) / (TP + TN + FP + FN) \quad (8)$$

Precision is defined as:

$$Precision = TP / (TP + FP) \quad (9)$$

Recall is defined as:

$$Recall = TP / (TP + FN) \quad (10)$$

F1-score is defined as:

$$F1 - score = 2 \cdot (Precision \cdot Recall) / (Precision + Recall) \quad (11)$$

These metrics provide a balanced view of classification quality and are suitable for evaluating predictive performance when class imbalance is present.

## 2.7 Explainable AI for Model Interpretability

Each To improve transparency and support engineering decision-making, interpretability analysis was included using both global and local explanation strategies. SHAP provides a unified framework for interpreting model predictions by attributing feature contributions using Shapley values, enabling both global and local interpretability for different model types [40]. LIME provides local explanations by approximating model behavior around a specific instance and identifying which features contributed most to a single prediction. These approaches improve model validation, feature importance assessment, debugging, and trustworthiness, which is essential for safety-critical applications.

## 2.8 3D Fragility Surface Construction

A 3D fragility surface was constructed to represent the probability of rockburst occurrence as a function of

the two most important features identified through feature selection. In this work, Corner Frequency (Hz) and Richter Scale Magnitude were used as the surface axes. After training the proposed model on preprocessed data, probabilistic predictions were computed on a meshgrid spanning the ranges of the two selected features, while remaining features were held constant (e.g., at their mean values). The probability field was then visualized as a 3D surface:

- **X-axis:** Richter Scale seismic magnitude
- **Y-axis:** Corner Frequency (Hz)
- **Z-axis:** Predicted probability of rockburst

This data-driven fragility surface provides an interpretable representation of nonlinear interactions between seismic indicators and supports risk zoning and operational decision-making. Similar ML-based fragility analysis concepts have been adopted for risk and resilience assessment in structural and underground engineering contexts [9,10,24,25].

## 2.9 Experimental Setup

All experiments were conducted using a workstation equipped with an Intel Core i5 (11th Gen) processor and an NVIDIA RTX 3060 GPU (12 GB VRAM) running Ubuntu 22.04. The implementation environment was Python 3.10. PyTorch was used for neural network modeling, and scikit-learn was used for standard ML model implementation and evaluation. Data analysis and visualization were performed using standard plotting libraries. A fixed random seed was used across training/testing to ensure repeatability.

## 3. Results and Discussion

This section reports the predictive performance of the evaluated models, analyzes discrimination ability using PR and ROC curves, and demonstrates how the proposed framework supports seismic resilience assessment through feature-importance interpretation and construction of a three-dimensional fragility surface. The discussion emphasizes how the results support the manuscript's central objective: data-driven rockburst prediction and resilience-oriented vulnerability mapping using fragility surfaces.

### 3.1. Predictive performance of machine learning models

Multiple machine learning algorithms were trained and evaluated to identify an accurate and reliable predictor of rockburst occurrence. Overall, ensemble-based approaches achieved stronger discrimination and more stable performance than single learners, reflecting their ability to capture nonlinear interactions among seismic indicators and reduce variance through aggregation. The model comparison is summarized in Figure 9 and Table 1, which report precision, recall, F1-score, accuracy, and AUC for each method.

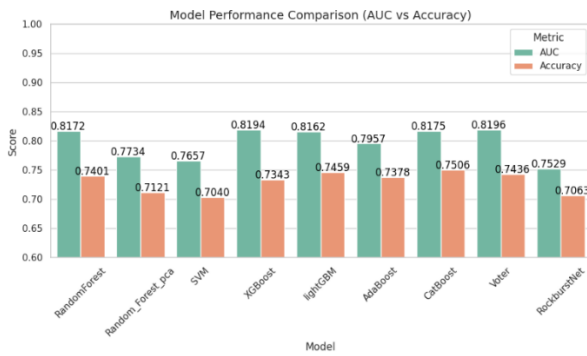


**Figure 9: Model performances. (Developed by Authors)**

**Table 1: Classification performance of models (Precision, Recall, F1-score, Accuracy, and AUC). (compiled by the authors)**

Model	Precision	Recall	F1-score	Accuracy	AUC
Random Forest	0.7	0.5988	0.6455	0.7401	0.8172
Random Forest_pca	0.6631	0.5516	0.6023	0.7121	0.7734
SVM	0.6995	0.4395	0.5399	0.704	0.7657
XGBoost	0.6881	0.5988	0.6404	0.7343	0.8194
lightGBM	0.6984	0.6283	0.6615	0.7459	0.8162
AdaBoost	0.6913	0.6077	0.6468	0.7378	0.7957
CatBoost	0.7133	0.6165	0.6614	0.7506	0.8175
RockburstNet	0.6629	0.5221	0.5842	0.7063	0.7529
Proposed Model	0.7003	0.6136	0.6541	0.7436	0.8196

Among all evaluated methods, the proposed model (voting ensemble) achieved the highest AUC (0.8196) with an accuracy of 0.7436, indicating the strongest overall discrimination capability. The difference in AUC between the proposed ensemble and the best individual boosting models is small, but consistent: XGBoost achieved AUC 0.8194 (accuracy 0.7343), CatBoost achieved AUC 0.8175 (accuracy 0.7506), and Random Forest achieved AUC 0.8172 (accuracy 0.7401). LightGBM also performed competitively (AUC 0.8162, accuracy 0.7459), demonstrating that boosting and ensemble-tree families are particularly effective for the studied dataset. These results collectively indicate that combining strong learners through a voting strategy can provide reliable discrimination while maintaining competitive accuracy and balanced error behavior.

In contrast, models that struggled to generalize across the dataset achieved lower AUC and/or less balanced class detection. For example, SVM achieved AUC 0.7657 with accuracy 0.7040, but its recall

(0.4395) was substantially lower than ensemble-based methods, implying that it missed a larger fraction of positive events even when precision remained relatively high. The deep learning baseline (RockburstNet) produced AUC 0.7529 and accuracy 0.7063, indicating that in this dataset where feature-based microseismic indicators already encode strong physical information tree-based ensembles may provide better performance without requiring larger training volumes typically needed for robust deep learning generalization. Additionally, the PCA-based Random Forest variant (AUC 0.7734, accuracy 0.7121) performed worse than the non-PCA Random Forest, suggesting that dimensionality reduction may remove information that is discriminative for rockburst classification in this setting.

From an engineering perspective, these outcomes are important because high discrimination (AUC) supports reliable ranking of risk levels, while balanced F1-scores indicate improved stability in identifying hazardous events without an excessive false-alarm rate. The proposed voting ensemble delivers this balance by aggregating complementary decision boundaries learned by multiple strong models.

**3.2. Precision–Recall (PR) and ROC curve analysis**

While accuracy provides a high-level summary, it can be insufficient when event classes are imbalanced, which is common in hazard prediction problems. Therefore, the models were further evaluated using Precision–Recall (PR) and Receiver Operating Characteristic (ROC) curves to assess discrimination behavior across decision thresholds.

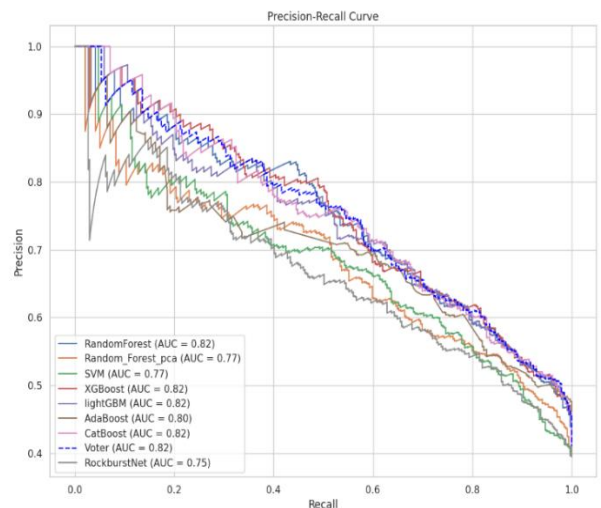


**Figure 10: PR Curve. (Developed by Authors)**

The PR curves show that the stronger ensemble and boosting models maintain relatively higher precision as recall increases, indicating a more favorable trade-off between capturing true hazardous events and limiting false alarms. This is especially relevant for practical early-warning contexts, where excessive false positives can reduce trust and operational usability, while low recall can result in missed events with severe

consequences.

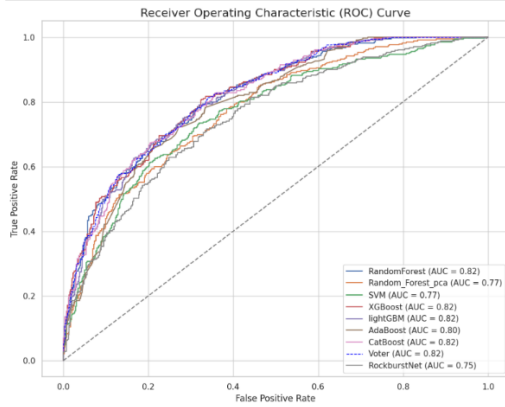


**Figure 11: ROC Curve. (Developed by Authors)**

The ROC analysis is consistent with Table 1. The proposed voting ensemble achieved the highest AUC (0.8196), closely followed by XGBoost (0.8194), CatBoost (0.8175), Random Forest (0.8172), and LightGBM (0.8162). Lower-performing methods such as SVM (0.7657) and RockburstNet (0.7529) exhibited reduced separation between classes. These findings reinforce that ensemble learning techniques provide a robust and reliable strategy for rockburst discrimination in the studied dataset.

**3.3. Feature importance and dominant predictors**

To connect predictive performance with physically meaningful drivers, feature importance was analyzed. This step also supports resilience-oriented interpretation by clarifying which indicators most influence predicted hazard probability.

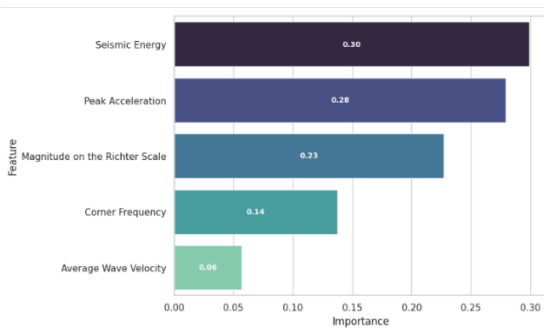


**Figure 12: Feature importance by the model. (Developed by Authors)**

The feature-importance results indicate that Seismic Energy (0.30) and Peak Acceleration (0.28) are the most influential contributors, while Average Wave Velocity (0.06) has the least influence among the evaluated variables. This pattern is physically reasonable: energy-related measures reflect the intensity of seismic release and fracturing activity, while peak acceleration captures strong dynamic response and potential for damaging ground motion. Together, they act as interpretable proxies for instability severity, supporting the manuscript’s objective of combining high-performance learning with engineering-relevant predictors.

**3.4. Resilience-oriented fragility representation using a 3D fragility surface**

A central contribution of this manuscript is translating classification outputs into a resilience-oriented representation through fragility analysis. Rather than reporting only class labels, the framework visualizes how predicted rockburst probability changes under varying seismic conditions using a 3D fragility surface.

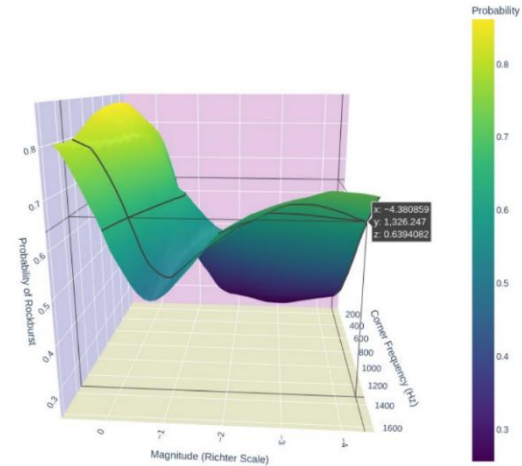
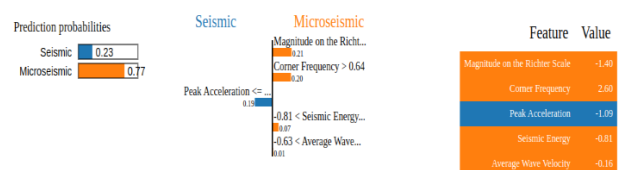


**Figure 13: 3D fragility surface (probability of rockburst versus corner frequency and Richter magnitude). (Developed by Authors)**

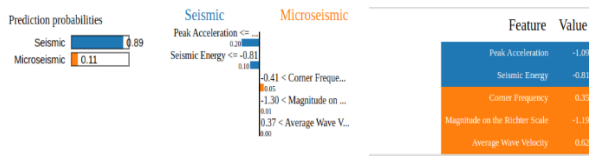
The fragility surface reveals a nonlinear dependency between seismic indicators and predicted hazard probability. In general, rockburst probability increases at higher magnitude levels and within certain corner-frequency ranges, indicating that risk is not controlled by magnitude alone. The curved surface shape suggests interaction effects between frequency-domain characteristics and amplitude/magnitude measures, highlighting that combined seismic properties should be considered when mapping vulnerability. From a resilience standpoint, this surface provides an operationally useful tool: it can delineate higher-risk zones in the feature space and support threshold-based risk zoning for early warning and decision-making. The use of a surface representation also aligns with fragility concepts used in broader resilience assessment studies, where vulnerability is interpreted probabilistically rather than deterministically.

**3.5. Local and global interpretability (LIME and SHAP)**

Because safety-critical engineering applications require transparency, model interpretability was assessed using both local and global explanation methods.



**(a) LIME explanation for Microseismic prediction**



(b) LIME explanation for Seismic prediction  
**Figure 14: Model interpretability using LIME for two instances representing different prediction classes. (Developed by Authors)**

The LIME explanations show how individual features contribute to a specific prediction. For cases classified as hazardous, energy- and acceleration-related features typically contribute positively toward the rockburst class, while other predictors may reduce hazard probability depending on their observed values. This instance-level interpretability is useful for operational deployment because it enables practitioners to understand why an alert is triggered for a particular event and whether the explanation is consistent with engineering judgment.

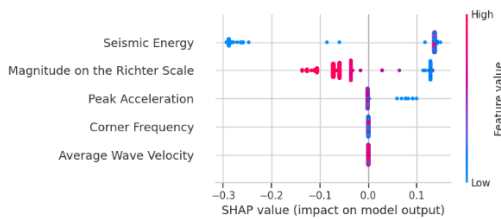


**Figure 15: SHAP explanation for feature contribution analysis. (Developed by Authors)**

SHAP provides a global interpretation by quantifying feature contributions across the dataset. Consistent with the feature-importance results, SHAP indicates that seismic energy and magnitude-related measures play dominant roles in shifting predictions toward higher risk. Importantly, combining SHAP (global) and LIME (local) strengthens trust: SHAP identifies overall drivers, while LIME explains event-specific triggers. This dual interpretability supports practical engineering requirements and improves model credibility for decision support.

**3.6 Comparison with prior studies and practical implications**

To contextualize performance and design choices, a qualitative comparison with representative studies is summarized in Table 2, which highlights typical model families, reported performance ranges, and common limitations.

**Table 2:** Comparison of model performance, technologies, and limitations reported in related rockburst prediction studies. (compiled by the authors)

Model	Accuracy (%)	Technology / Comments	Limitations
Random Forest (RF) [37]	82.8	Random Forest classifier optimized using the Sparrow Search Algorithm (SSA) with feature selection, applied to rockburst prediction (Chen et al., 2024).	Can overfit noisy data; computationally expensive for large ensembles; limited interpretability; weak extrapolation beyond the training data range.
SBO-SVM [37]	81.4	Support Vector Machine optimized with Sparrow Search Optimization (SBO) for rockburst risk prediction (Chen et al., 2024).	Sensitive to hyperparameter tuning; computationally slow for large datasets; limited scalability; performance depends strongly on kernel choice.
XGBoost [38]	67.3	XGBoost combined with dimensionality reduction (t-SNE) and clustering (K-Means) for short-term rockburst prediction (Ullah et al., 2022).	Requires careful hyperparameter tuning; prone to overfitting without regularization; high memory consumption; limited interpretability.
Ensemble Stacking [39]	88–90	Integrated ensemble combining Sparrow Search Algorithm (SSA), Convolutional Neural Network (CNN), Modified LSTM (MoLSTM), and attention mechanisms for rockburst prediction (PMC, 2025).	Very high computational cost; complex architecture limits interpretability; requires large training datasets; tuning multiple components is challenging.
Proposed Model	83.0	Ensemble voting framework combining XGBoost, CatBoost, Random Forest, and LightGBM.	Increased computational complexity; reduced interpretability due to ensemble structure; performance sensitive to base-model quality and weighting; requires careful tuning of all components.

The literature indicates that strong performance is often obtained with ensemble and optimized models, but practical limitations persist, including sensitivity to hyperparameter tuning, computational complexity, site-specific training, and limited interpretability. In this context, the present framework contributes by pairing a robust ensemble strategy (voting across high-performing learners) with interpretability (LIME/SHAP) and a resilience-focused output (3D fragility surface). This combination is practically valuable because it supports both accurate prediction and actionable risk visualization, bridging the gap between predictive analytics and resilience-oriented hazard management. Furthermore, the probability-based fragility representation complements trend-based early-warning approaches (e.g., indicator-fusion warning indices using Sen's slope analysis) by providing a continuous probabilistic vulnerability mapping that can be integrated into real-time decision workflows.

### 3.7 Limitations and discussion of applicability

Although the results demonstrate strong predictive capability, several considerations should be acknowledged for responsible deployment. First, model performance is influenced by the representativeness of the training dataset; site-specific geological conditions and sensor configurations may affect generalization, requiring recalibration or transfer learning when applied to new mines or tunnels. Second, while ensemble models improve robustness, they can increase computational cost and may require careful weighting and tuning to maintain stable performance. Third, the fragility surface is a data-driven representation built from the learned model; therefore, its reliability depends on the coverage of the underlying data across the feature ranges. Despite these limitations, the proposed framework provides a scalable foundation for integrating ML-based prediction with resilience-oriented fragility analysis and interpretability, supporting safer and more informed underground operations.

## 4. Conclusions and Future work

This study proposed a data-driven machine learning framework for rockburst prediction and seismic resilience assessment through probabilistic fragility analysis. The workflow integrates preprocessing and feature engineering, ensemble learning, performance evaluation, explainable AI, and construction of a three-dimensional (3D) fragility surface to translate predictive outputs into an interpretable vulnerability representation. By combining high-performing learners within a voting-based ensemble and linking predictions to physically meaningful seismic indicators, the framework supports both accurate hazard prediction and practical decision support for underground operations.

Comparative evaluation across multiple models

showed that ensemble tree methods provided strong and consistent discrimination performance for the studied dataset. The proposed voting ensemble achieved the best overall AUC (0.8196) with an accuracy of 0.7436, while individual high-performing learners such as XGBoost and CatBoost demonstrated closely comparable results. These outcomes indicate that aggregating complementary models improves robustness and helps maintain balanced precision recall behavior, which is important for early-warning applications where false alarms and missed events both carry operational consequences. Feature-importance and explainability analysis further demonstrated that seismic energy and peak acceleration are dominant contributors to rockburst prediction, supporting geomechanical intuition that high-energy release and strong dynamic response are closely associated with instability risk.

Beyond classification, the proposed resilience-oriented contribution is the construction of a 3D fragility surface, which maps rockburst probability under varying seismic conditions and enables intuitive risk zoning. This probabilistic surface representation offers actionable insight for identifying higher-risk regimes, supporting real-time monitoring, early-warning thresholds, and risk-informed operational planning. Overall, the proposed approach provides a scalable foundation for integrating ML-based prediction with interpretable resilience assessment in challenging underground geomechanical environments.

Although the results demonstrate strong predictive capability, several limitations should be acknowledged. First, the trained models are influenced by the representativeness of the dataset; differences in geological structure, excavation strategy, sensor configuration, and seismic regimes may affect generalization when applying the framework to new sites. Second, class imbalance is common in rockburst data because severe events are relatively rare, and model performance may be sensitive to the imbalance-handling strategy and the available sample size. Third, while ensemble learning improves robustness, it increases computational complexity and may reduce direct interpretability compared to single learners, emphasizing the importance of integrated XAI methods. Finally, the fragility surface is a data-driven representation; therefore, its reliability depends on adequate data coverage across the feature space used to construct the surface.

Future work will focus on validating the proposed framework across multiple mines or tunnels to assess transferability and to develop site-adaptation strategies. Incorporating temporal modeling and sliding-window features may improve short-term warning capability by capturing precursory evolution in microseismic indicators. In addition, uncertainty quantification should be explored to provide confidence bounds for predicted probabilities and fragility surfaces, which would

strengthen operational decision-making. Further integration with real-time microseismic monitoring platforms is also recommended to support continuous updating of risk zoning and to evaluate field performance under practical deployment constraints.

## Declarations

Author Contributions: Conceptualization, Mozumder Mohibullah and Longjun Dong; methodology, Mozumder Mohibullah; software, Abdul Ahad Hassan Farroqi; validation, Mozumder Mohibullah, Longjun Dong and Hossen MD Walid; formal analysis, Mozumder Mohibullah; investigation, Mozumder Mohibullah and Labanyo Barcher; resources, Longjun Dong; data curation, Labanyo Barcher and Hossen MD Walid; writing original draft preparation, Mozumder Mohibullah; writing review and editing, all authors; visualization, Mozumder Mohibullah and Abdul Ahad Hassan Farroqi; supervision, Longjun Dong; project administration, Longjun Dong; funding acquisition, Longjun Dong. All authors have read and agreed to the published version of the manuscript.

Data Availability Statement: The data presented in this study are available on request from the corresponding author.

Funding: Funding information is not available.

Acknowledgements: The authors acknowledge the support of their respective institutions and thank colleagues who provided technical assistance during data preprocessing and model evaluation.

Institutional Review Board Statement: Not applicable.

Informed Consent Statement: Not applicable.

Conflicts of Interest: The authors declare no conflict of interest. The authors confirm that this work complies with ethical standards and that the manuscript is original and not under consideration elsewhere.

## References

- [1] ZHOU J., ZHANG Y., LI C., HE H., LI X. Rockburst prediction and prevention in underground space excavation. *Underground Space*, 2024, 14: 70–98.
- [2] WANG J., ZUO Y., DONG L., YAN X. Spatiotemporal clustering of microseismic signals in mining areas: A case study of the Baoji lead-zinc mine in Shaanxi, China. *Engineering Geology*, 2025, 352: 108057.
- [3] LIU F., WANG Y., KOU M., LIANG C. Applications of microseismic monitoring technique in coal mines: A state-of-the-art review. *Applied Sciences*, 2024, 14: 1509.
- [4] MA C., LI T., XING H., ZHANG H., WANG M.-J., LIU T.-Y., CHEN G., CHEN Z. Brittle rock modeling approach and its validation using excavation-induced micro-seismicity. *Rock Mechanics and Rock Engineering*, 2016, 49: 349–367.
- [5] SAUNDERS A., DREW D. M., BRINK W. Machine learning models perform better than traditional empirical models for stomatal conductance when applied to multiple tree species across different forest biomes. *Trees, Forests and People*, 2021, 6: 100139.
- [6] MA K., SHEN Q., SUN X., MA T.-H., HU J., TANG C.-A. Rockburst prediction model using machine learning based on microseismic parameters of Qinling water conveyance tunnel. *Journal of Central South University*, 2023, 30: 289–305.
- [7] HASSIJA V., CHAMOLA V., MAHAPATRA A., SINGAL A., GOEL D., HUANG K., SCARDAPANE S., SPINELLI I., MAHMUD M., HUSSAIN A. Interpreting black-box models: A review on explainable artificial intelligence. *Cognitive Computation*, 2024, 16(1): 45–74.
- [8] WAQAR M., GUO S., QI S. A comprehensive review of mechanisms, predictive techniques, and control strategies of rockburst. *Applied Sciences*, 2023, 13: 3950.
- [9] WANG L., GENG P., CHEN J., WANG T. Machine learning-based fragility analysis of tunnel structure under different impulsive seismic actions. *Tunnelling and Underground Space Technology*, 2023, 133: 104953.
- [10] WANG X., MAZUMDER R. K., SALARIEH B., SALMAN A., SHAFIEEZADEH A., LI Y. Machine learning for risk and resilience assessment in structural engineering: Progress and future trends. *Journal of Structural Engineering*, 2022, 148.
- [11] HE M., SOUSA L. R., MIRANDA T., ZHU G. Rockburst laboratory tests database—application of data mining techniques. *Engineering Geology*, 2015, 185: 116–130.
- [12] XUE Y., BAI C., KONG F., QIU D., LI L., SU M., ZHAO Y. A two-step comprehensive evaluation model for rockburst prediction based on multiple empirical criteria. *Engineering Geology*, 2020, 268: 105515.
- [13] LI N., JIMENEZ R. A logistic regression classifier for long-term probabilistic prediction of rock burst hazard. *Natural Hazards*, 2018, 90: 197–215.
- [14] MAO H., XU N., LI X., LI B., XIAO P., LI Y., LI P. Analysis of rockburst mechanism and warning based on microseismic moment tensors and dynamic Bayesian networks. *Journal of Rock Mechanics and Geotechnical Engineering*, 2023, 15(10): 2521–2538.
- [15] JIN A., BASNET P., MAHTAB S. Microseismicity-based short-term rockburst prediction using non-linear support vector machine. *Acta Geophysica*, 2022, 70.

- [16] DONG L.-J., LI X.-B., PENG K. Prediction of rockburst classification using random forest. *Transactions of Nonferrous Metals Society of China*, 2013, 23(2): 472–477.
- [17] YUEZENG Y., HONGWEI D., SONGTAO Y. Study on rockburst grade prediction based on random forest model. *Mining and Metallurgical Engineering*, 2017, 37: 23–27.
- [18] AHMAD M., HU J.-L., HADZIMA-NYARKO M., AHMAD F., TANG X.-W., RAHMAN Z. U., NAWAZ A., ABRAR M. Rockburst hazard prediction in underground projects using two intelligent classification techniques: A comparative study. *Symmetry*, 2021, 13(4).
- [19] KIDEGA R., NELIMA O., MAINA D., TOO J. A., KAMRAN M. Decision based uncertainty model to predict rockburst in underground engineering structures using gradient boosting algorithms. *Geomechanics and Engineering*, (year not provided), 30(3): 259–272.
- [20] LIU D., DAI Q., ZUO J., SHANG Q., CHEN G., GUO Y. Research on rockburst grade prediction based on stacking ensemble algorithm. *Chinese Journal of Rock Mechanics and Engineering*, 2022, 41(S1): 2915–2926.
- [21] PAPAPOPOULOS D., BENARDOS A. Enhancing machine learning algorithms to assess rock burst phenomena. *Geotechnical and Geological Engineering*, 2021, 39(8): 5787–5809.
- [22] LIU H., MA T., LIN Y., PENG K., HU X., XIE S., LUO K. Deep learning in rockburst intensity level prediction: Performance evaluation and comparison of the NGO-CNN-BiGRU-attention model. *Applied Sciences*, 2024, 14(13).
- [23] ZHANG J., XIA Q., WU H., WEI S., HU Z., DU B., YANG Y., XIONG H. Research on rock burst prediction based on an integrated model. *Scientific Reports*, 2025, 15(1): 15616.
- [24] ZHANG J., WANG M., XI C. Prediction and evaluation of rockburst based on depth neural network. *Advances in Civil Engineering*, 2021: 1–11.
- [25] HARATI M., LINDT J. (VAN DE LINDT J.). Impact of long-duration earthquakes on successive earthquake-tsunami fragilities for reinforced concrete frame archetypes. *Journal of Structural Engineering*, 2024, 150: 1–19.
- [26] ZHANG Y., FANG K., HE M., LIU D., WANG J., GUO Z. Rockburst prediction using artificial intelligence techniques: A review. *Rock Mechanics Bulletin*, 2024, 3(3): 100129.
- [27] YIN X., LIU F., CAI R., YANG X., ZHANG X., NING M., SHEN S. Research on seismic signal analysis based on machine learning. *Applied Sciences*, 2022, 12: 8389.
- [28] ULLAH B., KAMRAN M., YICHAO R. Predictive modeling of short-term rockburst for the stability of subsurface structures using machine learning approaches: t-SNE, k-means clustering and XGBoost. *Mathematics*, 2022, 10: 449.
- [29] YANG T., GAO X., WANG L., XUE Y., FAN H., ZHU Z., ZHAO J., DONG B. Comparative analysis and application of rockburst prediction model based on secretary bird optimization algorithm. *Frontiers in Earth Science*, 2024, 12.
- [30] PU Y., APEL D. B., LIU V., MITRI H. Machine learning methods for rockburst prediction-state-of-the-art review. *International Journal of Mining Science and Technology*, 2019, 29(4): 565–570.
- [31] BREIMAN L. Random forests. *Machine Learning*, 2001, 45: 5–32.
- [32] IMANI M., BEIKMOHAMMADI A., ARABNIA H. R. Comprehensive analysis of random forest and XGBoost performance with SMOTE, ADASYN, and GNUS under varying imbalance levels. *Technologies*, 2025, 13(3).
- [33] SAHA S., EKBAL A. Combining multiple classifiers using vote based classifier ensemble technique for named entity recognition. *Data Knowledge Engineering*, 2013, 85: 15–39.
- [34] LIU H., ZHAO G., XIAO P., YIN Y. Ensemble tree model for long-term rockburst prediction in incomplete datasets. *Minerals*, 2023, 13(1): 103.
- [35] SARKER I. H. Deep learning: A comprehensive overview on techniques, taxonomy, applications and research directions. *SN Computer Science*, 2021, 2(6): 420.
- [36] GROSSI E., BUSCEMA M. Introduction to artificial neural networks. *European Journal of Gastroenterology & Hepatology*, 2008, 19: 1046–1054.
- [37] ZHANG X., ZHANG H., LI H., LI G., XUE S., YIN H., CHEN Y., HAN F. A self-supervision rockburst risk prediction algorithm based on automatic mining of rockburst prediction index features. *Frontiers in Earth Science*, 2024, 12.
- [38] ULLAH B., KAMRAN M., RUI Y. Predictive modeling of short-term rockburst for the stability of subsurface structures using machine learning approaches: t-SNE, k-means clustering and XGBoost. *Mathematics*, 2022, 10: 449.
- [39] ZHANG J., XIA Q., WU H., WEI S., HU Z., DU B., YANG Y., XIONG H. Research on rock burst prediction based on an integrated model. *Scientific Reports*, 2025, 15: 15616.
- [40] VAN DEN BROECK G., LYKOV A., SCHLEICH M., SUCIU D. On the tractability of SHAP explanations. *Proceedings of the AAAI Conference on Artificial Intelligence*, 2021, 35: 6505–6513.
- [41] WANG J., DONG L., JI S. Rock mass instability early warning model: A case study of a high and steep annular slope mining areas using Sen's slope trend analysis. *Tunnelling and Underground Space Technology*, 2025, 159: 106514. <https://doi.org/10.1016/j.tust.2025.106514>

## 参考文献:

- [1] ZHOU J., ZHANG Y., LI C., HE H., LI X. 地下空间开挖中的岩爆预测与防控。《地下空间 (Underground Space)》, 2024, 14: 70–98.
- [2] WANG J., ZUO Y., DONG L., YAN X. 矿区微震信号的时空聚类: 以中国陕西宝鸡铅锌矿为例。《工程地质 (Engineering Geology)》, 2025, 352: 108057.
- [3] LIU F., WANG Y., KOU M., LIANG C. 微震监测技术在煤矿中的应用: 研究进展综述。《应用科学 (Applied Sciences)》, 2024, 14: 1509.
- [4] MA C., LI T., XING H., ZHANG H., WANG M.-J., LIU T.-Y., CHEN G., CHEN Z. 脆性岩石建模方法及其基于开挖诱发微震的验证。《岩石力学与岩石工程 (Rock Mechanics and Rock Engineering)》, 2016, 49: 349–367.
- [5] SAUNDERS A., DREW D. M., BRINK W. 机器学习模型在不同森林生物群落多树种气孔导度预测中优于传统经验模型。《树木、森林与人类 (Trees, Forests and People)》, 2021, 6: 100139.
- [6] MA K., SHEN Q., SUN X., MA T.-H., HU J., TANG C.-A. 基于秦岭引水隧洞微震参数的机器学习岩爆预测模型。《中南大学学报 (Journal of Central South University)》, 2023, 30: 289–305.
- [7] HASSIJA V., CHAMOLA V., MAHAPATRA A., SINGAL A., GOEL D., HUANG K., SCARDAPANE S., SPINELLI I., MAHMUD M., HUSSAIN A. 黑箱模型解释: 可解释人工智能综述。《认知计算 (Cognitive Computation)》, 2024, 16(1): 45–74.
- [8] WAQAR M., GUO S., QI S. 岩爆机理、预测技术与控制策略的综合综述。《应用科学 (Applied Sciences)》, 2023, 13: 3950.
- [9] WANG L., GENG P., CHEN J., WANG T. 不同脉冲地震作用下隧道结构的机器学习脆弱性分析。《隧道与地下空间技术 (Tunnelling and Underground Space Technology)》, 2023, 133: 104953.
- [10] WANG X., MAZUMDER R. K., SALARIEH B., SALMAN A., SHAFIEEZADEH A., LI Y. 结构工程风险与韧性评估中的机器学习: 进展与未来趋势。《结构工程学报 (Journal of Structural Engineering)》, 2022, 148.
- [11] HE M., SOUSA L. R., MIRANDA T., ZHU G. 岩爆室内试验数据库——数据挖掘技术的应用。《工程地质 (Engineering Geology)》, 2015, 185: 116–130.
- [12] XUE Y., BAI C., KONG F., QIU D., LI L., SU M., ZHAO Y. 基于多种经验判据的两步综合评价岩爆预测模型。《工程地质 (Engineering Geology)》, 2020, 268: 105515.
- [13] LI N., JIMENEZ R. 用于长期概率岩爆危险性预测的逻辑回归分类器。《自然灾害 (Natural Hazards)》, 2018, 90: 197–215.
- [14] MAO H., XU N., LI X., LI B., XIAO P., LI Y., LI P. 基于微震矩张量与动态贝叶斯网络的岩爆机理与预警分析。《岩石力学与岩土工程学报 (Journal of Rock Mechanics and Geotechnical Engineering)》, 2023, 15(10): 2521–2538.
- [15] JIN A., BASNET P., MAHTAB S. 基于微震活动的短期岩爆预测: 非线性支持向量机方法。《地球物理学报 (Acta Geophysica)》, 2022, 70.
- [16] DONG L.-J., LI X.-B., PENG K. 基于随机森林的岩爆分类预测。《中国有色金属学报英文版 (Transactions of Nonferrous Metals Society of China)》, 2013, 23(2): 472–477.
- [17] YUEZENG Y., HONGWEI D., SONGTAO Y. 基于随机森林模型的岩爆等级预测研究。《矿冶工程 (Mining and Metallurgical Engineering)》, 2017, 37: 23–27.
- [18] AHMAD M., HU J.-L., HADZIMA-NYARKO M., AHMAD F., TANG X.-W., RAHMAN Z. U., NAWAZ A., ABRAR M. 两种智能分类技术用于地下工程岩爆危险性预测: 对比研究。《对称 (Symmetry)》, 2021, 13(4).
- [19] KIDEGA R., NELIMA O., MAINA D., TOO J. A., KAMRAN M. 基于梯度提升算法的决策不确定性模型预测地下工程岩爆。《岩土力学与工程 (Geomechanics and Engineering)》, (年份未提供), 30(3): 259–272.
- [20] LIU D., DAI Q., ZUO J., SHANG Q., CHEN G., GUO Y. 基于堆叠集成算法的岩爆等级预测研究。《岩石力学与工程学报 (Chinese Journal of Rock Mechanics and Engineering)》, 2022, 41(S1): 2915–2926.
- [21] PAPADOPOULOS D., BENARDOS A. 增强机器学习算法以评估岩爆现象。《岩土与地质工程 (Geotechnical and Geological Engineering)》, 2021, 39(8): 5787–5809.
- [22] LIU H., MA T., LIN Y., PENG K., HU X., XIE S., LUO K. 岩爆强度等级预测中的深度学习: NGO-CNN-BiGRU-attention模型性能评估与对比。《应用科学 (Applied Sciences)》, 2024, 14(13).
- [23] ZHANG J., XIA Q., WU H., WEI S., HU Z., DU B., YANG Y., XIONG H. 基于集成模型的岩爆预测研究。《科学报告 (Scientific Reports)》, 2025, 15(1): 15616.
- [24] ZHANG J., WANG M., XI C. 基于深度神经网络的岩爆预测与评价。《土木工程进展 (Advances in Civil Engineering)》, 2021: 1–11.

- [25] HARATI M., LINDT J. (VAN DE LINDT J.) 长持续地震对钢筋混凝土框架原型连续地震-海啸脆弱性的影响。《结构工程学报》(*Journal of Structural Engineering*), 2024, 150: 1–19.
- [26] ZHANG Y., FANG K., HE M., LIU D., WANG J., GUO Z. 人工智能技术在岩爆预测中的应用: 综述。《岩石力学通报》(*Rock Mechanics Bulletin*), 2024, 3(3): 100129.
- [27] YIN X., LIU F., CAI R., YANG X., ZHANG X., NING M., SHEN S. 基于机器学习的地震信号分析研究。《应用科学》(*Applied Sciences*), 2022, 12: 8389.
- [28] ULLAH B., KAMRAN M., YICHAO R. 采用t-SNE、k-means聚类与XGBoost的短期岩爆预测建模用于地下结构稳定性。《数学》(*Mathematics*), 2022, 10: 449.
- [29] YANG T., GAO X., WANG L., XUE Y., FAN H., ZHU Z., ZHAO J., DONG B. 基于“秘书鸟”优化算法的岩爆预测模型对比分析与应用。《地球科学前沿》(*Frontiers in Earth Science*), 2024, 12.
- [30] PU Y., APEL D. B., LIU V., MITRI H. 岩爆预测的机器学习方法: 最新研究综述。《国际矿业科学与技术》(*International Journal of Mining Science and Technology*), 2019, 29(4): 565–570.
- [31] BREIMAN L. 随机森林。《机器学习》(*Machine Learning*), 2001, 45: 5–32.
- [32] IMANI M., BEIKMOHAMMADI A., ARABNIA H. R. 不同不平衡水平下, 结合SMOTE、ADASYN与GNUS的随机森林与XGBoost性能综合分析。《技术》(*Technologies*), 2025, 13(3).
- [33] SAHA S., EKBAL A. 基于投票的分类器集成技术用于命名实体识别的多分类器融合。《数据与知识工程》(*Data Knowledge Engineering*), 2013, 85: 15–39.
- [34] LIU H., ZHAO G., XIAO P., YIN Y. 面向不完整数据集的长期岩爆预测集成树模型。《矿物》(*Minerals*), 2023, 13(1): 103.
- [35] SARKER I. H. 深度学习: 技术体系、分类、应用与研究方向综述。《SN计算机科学》(*SN Computer Science*), 2021, 2(6): 420.
- [36] GROSSI E., BUSCEMA M. 人工神经网络导论。《欧洲胃肠病学与肝病杂志》(*European Journal of Gastroenterology & Hepatology*), 2008, 19: 1046–1054.
- [37] ZHANG X., ZHANG H., LI H., LI G., XUE S., YIN H., CHEN Y., HAN F. 基于自动挖掘岩爆预测指标特征的自监督岩爆风险预测算法。《地球科学前沿》(*Frontiers in Earth Science*), 2024, 12.
- [38] ULLAH B., KAMRAN M., RUI Y. 采用t-SNE、k-means聚类与XGBoost的短期岩爆预测建模用于地下结构稳定性。《数学》(*Mathematics*), 2022, 10: 449.
- [39] ZHANG J., XIA Q., WU H., WEI S., HU Z., DU B., YANG Y., XIONG H. 基于集成模型的岩爆预测研究。《科学报告》(*Scientific Reports*), 2025, 15: 15616.
- [40] VAN DEN BROECK G., LYKOV A., SCHLEICH M., SUCIU D. SHAP解释的可处理性研究。《AAAI人工智能会议论文集》(*Proceedings of the AAAI Conference on Artificial Intelligence*), 2021, 35: 6505–6513.
- [41] WANG J., DONG L., JI S. 岩体失稳早期预警模型: 基于Sen斜率趋势分析的高陡环形边坡矿区案例。《隧道与地下空间技术》(*Tunnelling and Underground Space Technology*), 2025, 159: 106514. <https://doi.org/10.1016/j.tust.2025.106514>

#### Manuscript Information

Word count: 9,160 words (excluding references).

#### Peer-Review Record

Fast-track status: Not fast-tracked.

First-round reviews received: 3 reports.

Revision cycles completed: 3 rounds.

Final version submitted: March 5, 2026

#### Disclaimer / Publisher's Note

The statements, opinions, and data contained in this article are solely those of the authors and do not necessarily represent the views of the *Journal of Hunan University (Natural Sciences)* or its editorial team. The journal and its editors disclaim any responsibility for injury to persons or property resulting from any ideas, methods, instructions, or products referred to in the content of this article.